Flexible OFDM schemes for bursty transmissions

Romain Couillet, Merouane Debbah

Flexible OFDM schemes for bursty transmissions

Romain Couillet
NXP Semiconductors, Sophia Antipolis
505 Route des Lucioles
06560 Sophia Antipolis, France
Email: romain.couillet@nxp.com

Mérouane Debbah
Alcatel-Lucent Chair, Supelec
Plateau de Moulon, 3 rue Joliot-Curie
91192 Gif sur Yvette, France
Email: merouane.debbah@supelec.fr

***Abstract*—In this paper, α-OFDM, a generalization of the OFDM modulation, is proposed to enhance the outage capacity of bursty transmissions. This new flexible modulation scheme is easily implemented and only requires a symbol rotation of angle α after the IDFT stage. The induced rotation slides the DFT window and provides frequency diversity in block fading channels. Interestingly, the results show a substantial gain in terms of outage capacity and BER in comparison with classical OFDM modulation schemes. The framework is extended to multiuser/multi-antenna OFDM based standards. Simulations, in the context of 3GPP LTE, called hereafter α-LTE, sustain our theoretical claims.**

I. Introduction

With the recent growth of wireless communications and the increasing demand for high transmission rates, Orthogonal Frequency Division Multiplexing (OFDM) is being considered the modulation scheme of most of the future wireless communication technologies. Many wireless standards [1]-[3] have already rallied in favour of OFDM. One attractive feature of OFDM is the *flat fading* aspect of the channel that facilitates the equalization process at the receiver side. This property originates from the *cyclic prefix* (CP) addition prior to signal transmission that allows to model the channel as a circulant matrix in the time-domain [7]. As circulant matrices are diagonalizable in the Fourier basis, the channel frequency response is seen as a set of orthogonal flat fading subchannels.

In addition to their demand for high transmission rates, recent wireless standards have also moved from the connected *circuit-switched* to the bursty *packet-switched* transmission mode. The main drawback of the *packet-switched* mode arises when the transmission time is less than the channel *coherence time* [11], as the channel is then static over the communication time. Indeed, for any target transmission rate R, there exists a non-null probability that the channel is so ill-conditioned that the resulting capacity is less than R. This outage probability is especially non negligible in OFDM when the channel delay spread is small, or equivalently when the channel *coherence bandwidth* [11] is large. These observations have led to consider methods which provide channel *diversity* to protect the transmitted symbols from deep channel fading. Among those methods, [5] proposed a dynamic beamforming scheme using multiple antennas, known as “dumb antennas”, which induces fast channel variations in time. The relevant effect of this method is to increase the channel diversity during the transmission period. Recently, [6] introduced a *compact MIMO* system which emulates many antennas from one single virtually rotating antenna, thus producing an additional degree of freedom. In [12], *cyclic delay diversity* was shown to trade space diversity for frequency diversity, thanks to different transmission delays introduced on a set of transmit antennas. However, all those methods require additional antennas to provide channel diversity.

In the following work, we propose first a new single antenna single user modulation scheme called α-OFDM, which exploits the full frequency diversity transmission band with no additional complexity. The main idea is to transmit on new carriers which have not been previously exploited. In particular, we show that α-OFDM allows to flexibly reuse adjacent frequency bands by properly adjusting a rotation parameter: α.

The work is then extended to the multi-user OFDMA (Multiple Access OFDM) case, where 3GPP-Long Term Evolution (LTE) is used as benchmark comparison. Although both α-LTE and LTE with frequency hopping techniques seem to be similar, the α-OFDM algorithm is more flexible and can be adapted on a per-OFDM symbol rate without advanced scheduling methods.

In both cases, the α-OFDM-based systems are compared against their classical OFDM system counterparts in their respective outage capacity and outage bit error rate (BER) performances.

The rest of the paper unfolds as follows: in section II, we study the mathematical extension of circulant matrices, which is at the heart of the α-OFDM modulation schemes and we introduce the novel α-OFDM modulation scheme. Practical system-level schemes based on α-OFDM are then presented in section III. The theoretical claims are validated by simulations in section IV. We then introduce in section V some practical applications and quantify the outage performance gain. In particular we propose an extension for the 3GPP LTE standard, called α-LTE. Finally, conclusions are provided in section VI.

Notations: In the following, boldface lower and capital case symbols represent vectors and matrices, respectively. The transposition is denoted $(\cdot)^{\mathsf{T}}$ and the Hermitian transpose is $(\cdot)^{\mathsf{H}}$. The operator $\mathrm{diag}(\mathbf{x})$ turns the vector $\mathbf{x}$ into a diagonal matrix. The symbol $\det(\mathbf{X})$ is the determinant of matrix $\mathbf{X}$. The symbol $\mathrm{E}[\cdot]$ denotes expectation. The binary relation symbol $X|Y$ means that Y is divisible by X. The notation $\mathbf{x} \xrightarrow{\mathcal{F}} \mathbf{y}$ means that $\mathbf{y}$ is the discrete Fourier transform of $\mathbf{x}$.

II. Model

A. Mathematical Preliminaries

Definition 1: For $z = \rho e^{i\alpha} \in \mathbb{C}$, $(\rho, \alpha) \in \mathbb{R}^+ \times \mathbb{R}$, we call an $N \times N$ matrix $\mathbf{H}$ (ρ, α)-circulant if it is of the form

$$\mathbf{H} = \begin{bmatrix} h_0 & 0 & \dots & 0 & \rho e^{i\alpha} h_{L-1} & \dots & \rho e^{i\alpha} h_1 \\ h_1 & h_0 & \ddots & & \ddots & \ddots & \vdots \\ \vdots & & \ddots & \ddots & & \ddots & \rho e^{i\alpha} h_{L-1} \\ h_{L-1} & & & \ddots & \ddots & & 0 \\ 0 & \ddots & & & \ddots & \ddots & \vdots \\ \vdots & \ddots & \ddots & & & h_0 & 0 \\ 0 & \dots & 0 & h_{L-1} & \dots & h_1 & h_0 \end{bmatrix}. \tag{1}$$

This is a matrix with first column $[h_0, \dots, h_{L-1}, 0, \dots, 0]^{\mathsf{T}}$, and subsequent columns are successive cyclic shifts of this column, with the upper triangular part of the matrix multiplied by $\rho e^{i\alpha}$.

Proposition 1: All $N \times N$ (ρ, α)-circulant matrices are diagonalizable by the (ρ, α)-Fourier matrix $\mathbf{F}_{N,(\rho,\alpha)}$, with

$$\mathbf{F}_{N,(\rho,\alpha)} = \mathbf{F}_N \cdot \mathrm{diag}\left(1, \rho^{\frac{1}{N}} e^{i\alpha\frac{1}{N}}, \dots, \rho^{\frac{N-1}{N}} e^{i\alpha\frac{N-1}{N}}\right) \tag{2}$$

Hence we denote

$$\mathrm{diag}\left(\phi_0, \dots, \phi_{N-1}\right) = \mathbf{F}_{N,(\rho,\alpha)} \mathbf{H} \mathbf{F}_{N,(\rho,\alpha)}^{-1} \tag{3}$$

where the diagonal elements are given by the (ρ, α)-DFT of the first column of $\mathbf{H}$

$$[\phi_0, \dots, \phi_{N-1}]^{\mathsf{T}} = \mathbf{F}_{N,(\rho,\alpha)} [h_0, \dots, h_{L-1}, 0, \dots, 0]^{\mathsf{T}} \tag{4}$$

The proof of proposition 1 is provided in [13].

B. OFDM

Consider a regular OFDM transmission scheme. Denote $\mathbf{s} \in \mathbb{C}^N$ the transmitted OFDM symbol, $\mathbf{n} \in \mathbb{C}^N$ the additive white Gaussian noise (AWGN) with entries of variance $\mathrm{E}[|n_i|^2] = \sigma^2$ and $\mathbf{H}$ the circulant time-domain channel matrix. The time-domain received signal $\mathbf{r} \in \mathbb{C}^N$ reads

$$\mathbf{r} = \mathbf{H}\mathbf{F}^{\mathsf{H}}\mathbf{s} + \mathbf{n} \tag{5}$$

where $\mathbf{F}_N$ is rewritten $\mathbf{F}$ for the sake of readability. Therefore $\mathbf{H}$ is diagonalizable by the Fourier matrix $\mathbf{F}$, with diagonal elements the discrete Fourier transform of the first column $[h_0, \dots, h_{L-1}, 0, \dots, 0]^{\mathsf{T}}$. This is simply obtained by multiplying $\mathbf{r}$ in (5) by $\mathbf{F}$. The distribution of the noise does not change, since a unitary transformation of a Gaussian vector is still a Gaussian vector. Thus,

$$\mathbf{F} \cdot \mathbf{r} = \mathrm{diag}\left(H(0), \dots, H\left(N-1\right)\right) \mathbf{s} + \mathbf{n} \tag{6}$$

with $H(\cdot)$ the DFT of the first column of $\mathbf{H}$,

$$H\left(m\right) = \sum_{j=0}^{L-1} h_j e^{-2\pi i j \frac{m}{N}} \tag{7}$$

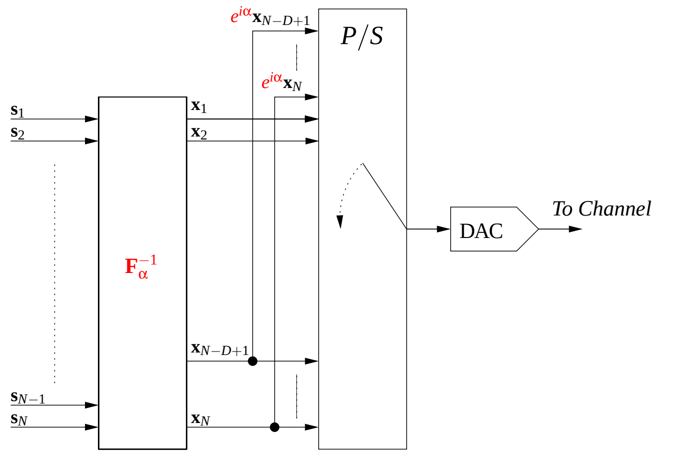

Fig. 1. α-OFDM transmission scheme

C. α-OFDM

The α-OFDM scheme consists in a first multiplication of the time-domain symbols of the CP by the constant $z = \rho e^{i\alpha}$ with $\rho = 1$. If ρ were chosen different from 1, $\mathbf{F}_{N,(\rho,\alpha)}$ would not be unitary, which would generate noise amplification at the receiver side. Then the time-domain OFDM signal is multiplied by the matrix $\mathrm{diag}\left(1, e^{-i\alpha/N}, \dots, e^{-i\alpha(N-1)/N}\right)$ after the inverse DFT (IDFT) process in the OFDM transmission chain. This is presented in figure 1. Thus α-OFDM introduces only a minor change compared to OFDM. Note that the classical OFDM modulation is the particular α-OFDM scheme for which $\alpha = 0$.

Hence, the time-domain received signal $\mathbf{r}$ is

$$\mathbf{r} = \mathbf{H}\mathbf{F}_\alpha^{\mathsf{H}}\mathbf{s} + \mathbf{n} \tag{8}$$

where $\mathbf{F}_\alpha$ is a simplified notation for $\mathbf{F}_{N,(1,\alpha)}$ and $\mathbf{H}$ is α-circulant (i.e. $\mathbf{H}$ is $(1, \alpha)$-circulant). $\mathbf{H}$ can then be diagonalized by $\mathbf{F}_\alpha$.

Discarding the CP and multiplying $\mathbf{r}$ by $\mathbf{F}_\alpha$ at the receiver, one has

$$\mathbf{F}_\alpha \cdot \mathbf{r} = \mathrm{diag}\left(\Phi_\alpha\left(0\right), \dots, \Phi_\alpha\left(N-1\right)\right) \mathbf{s} + \mathbf{n} \tag{9}$$

with $\Phi_\alpha(\cdot)$ the α-DFT of the first column of $\mathbf{H}$:

$$\Phi_\alpha\left(m\right) = \sum_{j=0}^{L-1} h_j e^{-2\pi i \frac{j}{N}\left(m - \frac{\alpha}{2\pi}\right)} \tag{10}$$

Note that $\Phi_\alpha(m)$ is a frequency shifted version of $H(m)$. Thus α-OFDM introduces a fractional *frequency shift* $\alpha/2\pi$ to the channel $\{H(0), \dots, H(L-1)\}$. Particularly, if $\alpha/2\pi$ is an integer, then α-OFDM merely remaps the OFDM symbol onto a circular-shifted version of the subcarriers.

III. Outage Capacity Analysis

A. Introduction

The transmission rates achievable in bursty communications cannot be evaluated with Shannon's formulation of the ergodic capacity which involves infinite delay data transmission.

Rather, the transmission capabilities of a bursty system are usually measured through the rate achievable $(100-q)\%$ of the time. This rate C_0 is known as the $q\%$-outage capacity and verifies $\mathbb{P}(C > C_0) = (100-q)/100$, with C the Shannon's capacity [4] for fixed channels.

B. α-OFDM capacity

The normalized capacity C of a regular OFDM system (also called *spectral efficiency*) for the fixed channel $\{H(0), \ldots, H(N-1)\}$ reads

$$C = \frac{1}{N} \sum_{m=0}^{N-1} \log\left(1 + \frac{|H(m)|^2}{\sigma^2}\right) \tag{11}$$

while the capacity for α-OFDM is

$$C_\alpha = \frac{1}{N} \sum_{m=0}^{N-1} \log\left(1 + \frac{|\Phi_\alpha(m)|^2}{\sigma^2}\right) \tag{12}$$

Remind that the channel *coherence bandwidth* of an OFDM system is at least as large as the subcarrier spacing (otherwise the channel delay spread would be longer than the OFDM symbol duration). Therefore, $\Phi_\alpha(m) \simeq H(\lceil \frac{\alpha}{2\pi} \rceil_N)$ where $\lceil x \rceil_N$ denotes the closest integer larger than x modulo N. From which we conclude that $C \simeq C_\alpha$. As a consequence, α-OFDM does not bring any gain, either in terms of ergodic or outage capacity.

Nonetheless, for various reasons, such as the introduction of frequency guard bands or oversampling at the receiver, many OFDM systems with a size-N DFT use a limited number of subcarriers $N_u \leq N$ to transmit data. Those are named *useful* subcarriers. In such schemes, one has

$$C = \frac{1}{N_u} \sum_{m=0}^{N_u-1} \log\left(1 + \frac{|H(m)|^2}{\sigma^2}\right) \tag{13}$$

As for α-OFDM, the capacity C_α is computed as

$$C_\alpha = \frac{1}{N_u} \sum_{m=0}^{N_u-1} \log\left(1 + \frac{|\Phi_\alpha(m)|^2}{\sigma^2}\right) \tag{14}$$

The size of the bandwidth of both OFDM and α-OFDM are the same but their location differs and therefore $C \neq C_\alpha$. This capacity would only make sense if the frequency guard bands are reusable and not protected, which is rarely the case in single user OFDM systems. However, we shall see in the subsequent sections that this apparent strong limitation can be released in specific scenarios. In the remaining of this paper, we therefore consider OFDM systems with N subcarriers transmitting data over N_u useful subcarriers whose locations are subject to different contraints.

C. α-OFDM-based systems

1) α-OFDM#1: First consider a single-user OFDM system with the $N - N_u$ non-useful subcarriers gathered into a contiguous subband, up to a circular rotation over the bandwidth. This loose constraint allows to use α-OFDM for any $\alpha \in \mathbb{R}$ as long as the N_u useful subcarriers are gathered in a contiguous band. We then naturally introduce the α-OFDM#1 scheme as follows.

Let $M \in \mathbb{N}$ some integer constant. α-OFDM#1 assumes that a particular set

$$\mathcal{M} = \left\{0, 2\pi\frac{N}{M}, \ldots, 2\pi\frac{N(M-1)}{M}\right\} \tag{15}$$

of M values for α is a priori known both to the transmitter and to the receiver. The symbols $\mathbf{s}$ are transmitted successively using a $(2\pi k/M)$-OFDM modulation, with k ranging from 1 to N, e.g. the first symbol $\mathbf{s}^{(1)}$ is sent using 0-OFDM, then $\mathbf{s}^{(2)}$ is sent using $(2\pi N/M)$-OFDM etc. At the receiver side, the corresponding α values are used to decode the received symbols.

The capacity $C_{\#1}$ of the α-OFDM#1 scheme is

$$C_{\#1} = \frac{1}{MN_u} \sum_{m=0}^{N_u-1} \sum_{\alpha \in \mathcal{M}} \log\left(1 + \frac{|\Phi_\alpha(m)|^2}{\sigma^2}\right). \tag{16}$$

2) α-OFDM#2: Assuming perfect channel state information at the transmitter (CSIT), an improved scheme, α-OFDM#2, can be derived from α-OFDM#1, which selects among the M values of $\mathcal{M}$ the one that maximizes the instantaneous capacity. Its capacity $C_{\#2}$ reads

$$C_{\#2} = \frac{1}{N_u} \max_{\alpha \in \mathcal{M}} \sum_{m=0}^{N_u-1} \log\left(1 + \frac{|\Phi_\alpha(m)|^2}{\sigma^2}\right). \tag{17}$$

3) α-OFDM#3: Consider now that the protected unused subcarriers can only be placed on the lowest frequency and highest frequency sides of the bandwidth. Following the same structure as the α-OFDM#1 scheme, we introduce α-OFDM#3, based on a set $\mathcal{M}$ of M values for α which are constrained by $N_u - N \leq \frac{\alpha}{2\pi} \leq N - N_u$. The introduction of this particular scheme is relevant as the basis for some practical applications studied in section V. The capacity formulation $C_{\#3}$ is identical to equation (16) with the additional constraint on the set of rotations $\mathcal{M}$. Therefore, $\max_{\mathcal{M}} C_{\#3}(\mathcal{M}) \leq \max_{\mathcal{M}} C_{\#1}(\mathcal{M})$.

D. Capacity Gain

The effect of the α-OFDM#n schemes is to slide the OFDM DFT window by different frequency shifts. This generates channel diversity that is highly demanded in outage scenarios. The following lemma shows that the *per subcarrier* fixed-channel capacity limit of α-OFDM#1, for any $N_u < N$, equals the *per subcarrier* fixed-channel capacity of an OFDM system, for $N_u = N$. The ratio between the total α-OFDM#1 capacity and the total OFDM capacity is then N_u/N for a proper choice of $\mathcal{M}$.

Lemma 1: Consider a single user OFDM system with N_u useful subcarriers and N total subcarriers without channel state information at the transmitter (CSIT). Apply α-OFDM#1 with a pattern $\mathcal{M}$ of cardinal M like in (15) with the constraint $N | \{M \cdot gcd(N, N_u)\}$, $gcd(x, y)$ being the greater common divider of x and y. Assuming the channel coherence time is

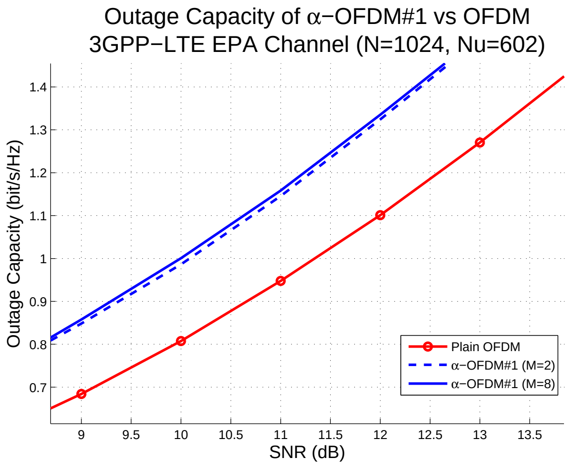

Fig. 2. α-OFDM#1 Outage Capacity in 3GPP-LTE EPA

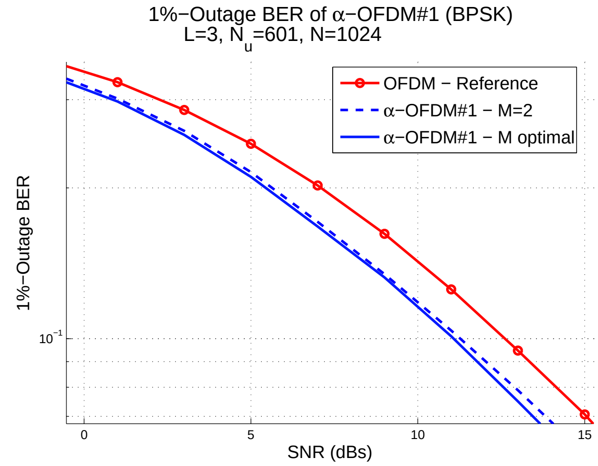

Fig. 3. α-OFDM#1 BER

more than M times the OFDM symbol duration, the capacity reads

$$C_{\#1} = \frac{1}{N}\sum_{m=0}^{N-1}\log\left(1+\frac{\left|H\left(\frac{m}{N}\right)\right|^2}{\sigma^2}\right) \qquad (18)$$

For a proof of lemma 1, refer to [13].

The achievable outage capacity for α-OFDM#3 being less than the outage capacity for α-OFDM#1, proposition 1 provides an upper bound on the achievable capacity for α-OFDM#3.

IV. Simulation and Results

The 3GPP-LTE OFDM standard is considered in most simulations. We present results for the 1.4 MHz bandwidth ($N_u = 76, N = 128$) and the 10MHz bandwidth ($N_u = 602, N = 1024$). In LTE, the null subcarriers on the bandwidth sides do not correspond to guard bands but are due to oversampling at the receiver; as a result, the $N - N_u$ empty subcarriers overlap the adjacent users' bands. We will study the outage capacity and BER gain assuming that we were allowed to slide the spectrum over those bands while still sending data on N_u circularly consecutive subcarriers. Channels are modeled either as exponential decaying with mean zero and unit variance or as LTE reference channels [9].

A. SISO case

Figure 2 compares the outage capacity gain of α-OFDM#1 against plain OFDM in LTE EPA channels for a set $\mathcal{M}$ of length $M = 2$ and $M = 8$. The bandwidth is 1.4 MHz. A strong SNR gain is provided by α-OFDM#1 already for $M = 2$ ($+1.1$ dB), while growing M does not bring significant improvement. This is explained by the fact that $M = 2$ suffices to transmit over all available subcarriers, providing already a high diversity gain. Note also that this gain is dependent on the channel length (it can be shown that α-OFDM#1 in EVA channels shows 1.3 dB gain while in ETU it does not overtake 0.4 dB gain).

In terms of outage BER, corresponding gains are shown in figure 3, which presents results obtained for BPSK signaling and MMSE decoding over Rayleigh fading channels with $M = 2$ or M chosen to optimize channel diversity. As previously stated, $M = 2$ already provides a significant gain, close to the limit with an ideal set $\mathcal{M}$.

B. Single User with multiple antennas

Figure 4 depicts the gain of α-OFDM schemes versus OFDM in Rayleigh channels using multiple antennas at the transmitter. It is observed that the usage of additional diversity antennas can be partially or fully replaced by α-OFDM schemes. Channel diversity from the space domain can then be traded off with diversity in the time-domain thanks to α-OFDM, at a minimal cost. However, particular care is required to appreciate those results, as the performance gains heavily depend on the outage percentage q as well as on the channel delay spread. In mobile short-range wireless communication schemes, bursty transmissions using α-OFDM can be transmitted at higher rates. This might efficiently replace additional antennas, meant to provide spatial diversity.

C. Multi-cell systems

In multi-cell systems, inter-cell interference engenders outage situations whenever the terminal's own cell shows bad channel conditions while the channel to the interferer is strong. Using α-OFDM in its own cell, not only will the terminal diversify its own channel but it will also face different interference patterns. Therefore, it is even less likely to simultaneously be confronted to bad channel conditions and strong interference over the consecutive M α-OFDM symbols. Figure 5 provides this analysis, in which a user faces interference under SNR $= 15$ dB and varying signal to interference ratio (SIR). The channel length is set to $L = 3$ while $N_u = 601$ and the DFT size is $N = 1024$. At high SIR, one finds again the α-OFDM capacity gain observed in figure 2. Around SIR $= 20$ dB, a level for which interference becomes a relevant factor, the outage gain due to α-OFDM#1

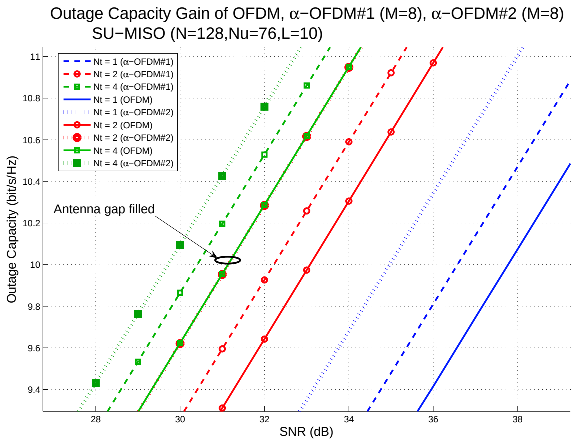

Fig. 4. Outage Capacity gain for α-OFDM MISO

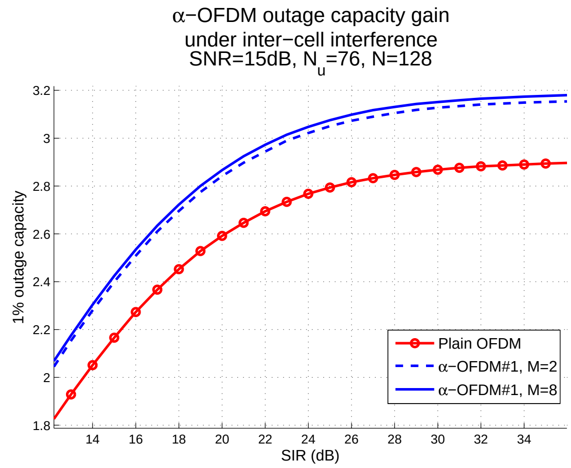

Fig. 5. α-OFDM#1 with intercell interference

is more than 3 dB, which is twice the capacity gain obtained in single-cell OFDM. As discussed in the previous section, those gains are even larger if the considered outage is less than 1% and is less for more frequency selective channels.

V. Applications

In this study, on the specific example of the 1.4 MHz LTE frequency band, we assumed that we were allowed to transmit data on extra frequency bands on the bandwidth edges to capitalize on channel diversity. This requires that those bands are not in use. In the following we propose schemes for service providers to overcome this problem by sacrificing a small part of the total bandwidth.

A. α-LTE

In the LTE context, service providers are allowed to use up to 20 MHz bandwidth that they can freely subdivide in several chunks. Consider that one decides to cut off the available bandwidth in 16 chunks of 1.25 MHz each. Those chunks are composed of 76 subcarriers which are oversampled to 128 for ease of computation at the transmitter and at the receiver. We propose to sacrifice an amount of 4 subcarriers per chunk that then results in a $4 \times 16 = 64$ free subcarriers in total. Those 64 subcarriers are gathered in two subbands of 32 subcarriers, placed on both sides of the 20 MHz band. By synchronously using α-OFDM on every chunk for a maximum of 16 users, we can design a system of $N_u = 76 - 4 = 72$ effective subcarriers per user over a total $N = 72 + 64 = 136$ available subcarriers. Indeed, the 64 spared subcarriers are reusable to every user by sliding their individual DFT windows.

Figure 7 illustrates a simplified version of the afore described scheme, with 4 chunks instead of 16. In this particular example, an $M = 3$ α-OFDM-based scheme is used that synchronously exploits the left subcarriers of the dotted part of each chunk, then the central subcarriers and finally the right subcarriers in any three consecutive OFDM symbols $(\mathbf{s}^{(3k)}, \mathbf{s}^{(3k+1)}, \mathbf{s}^{(3k+2)})$. Therefore, data will always be sent on individual and non-overlapping bandwidths. In our particular example, we use a 136-DFT for a signal occupying the central 72-subcarrier band.

The gain of α-LTE lies in outage BER and also, at a low-to-medium SNR, in outage capacity. Indeed, the lack of 4 subcarriers introduces a factor $72/76$ on the total outage capacity C derivation that scales like $N_u \log(SNR)$ at high SNR. But at low-to-medium SNR, the gain discussed in section III appears and overtakes the loss in outage capacity introduced by the lost 4 subcarriers. The outage BER also shows better performance than the former OFDM system, which translates into a constant SNR gain at medium-to-high SNR.

Figure 6 provides the simulation results obtained in 1% outage capacity for a transmission through 3GPP-EVA channels with $N_u = 72$, $N = 136$ in the low-to-medium SNR regime. For fair comparison, we plotted the outage capacity cumulated over a bandwidth of 76 subcarriers (therefore, when $N_u = 72$, 4 subcarriers are left unused) that we normalize by 76. As stated before, at low-to-medium SNR, a gain in capacity is observed, despite the loss of 4 subcarriers. At high SNR, we can observe that the classical OFDM fills the gap with our improved method. The position of the crossing point depends in particular on the channel delay spread and on the channel coherence time. This is another compromise to take into consideration for a precise utilization of α-OFDM.

B. Ultra-Wide Band

3GPP LTE is not the only standard to allow its allocated bandwidth to be divided into many OFDM systems. For instance, UWB systems, that cannot manage very large DFT computations, divide their allocated bandwidth into multiple OFDM chunks. α-LTE can be generalized to systems of total bandwidth $\mathcal{W}$ with N subcarriers, subdivided into K subbands. In classical OFDM, this results in chunks of size N/K and therefore, without oversampling, to a DFT size N/K.

With α-OFDM, one can introduce a guard band of G subcarriers, to result into K chunks of size $(N-G)/K$ and to an $((N-G)/K + G)$ DFT size. By making (N, K) grow to

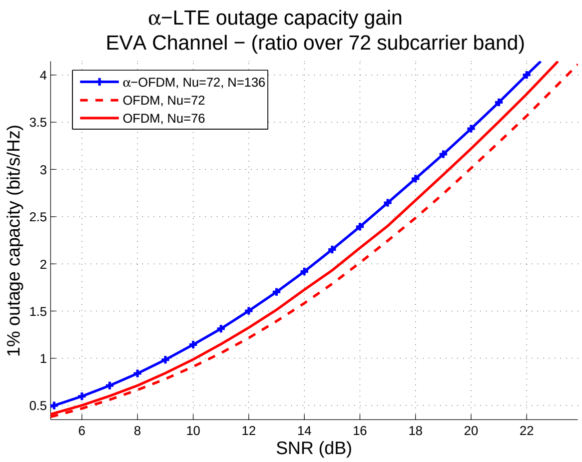

Fig. 6. LTE & α-LTE outage capacity

infinity with a constant ratio, the DFT size tends to $(N/K+G)$ while the number of useful subcarriers is fixed to N/K.

The loss in outage capacity per chunk at high SNR is then fairly reduced while the gain in outage BER per chunk is kept constant independently of (N, K). In this limit scenario, α-OFDM does not require to sacrifice bandwidth but provides diversity and outage capacity gain.

C. *Cognitive Radios in Unlicensed Bands*

Advanced techniques of channel sensing allow cognitive radios [10] to figure out the spectral occupation of the neighbouring frequencies. For bursty systems, it could be convenient to reuse this free sensed bandwidth $\mathcal{W}_e$. By increasing the rotation pattern $\mathcal{M}$ accordingly, for instance $\mathcal{M} = \{0, 2\pi N\mathcal{W}_e/\mathcal{W}\}$, it is possible to dynamically gain in channel diversity. The terminal can be dynamically informed of the mode to be used in a few bits through a dedicated control channel.

VI. Conclusion

In this paper, flexible OFDM schemes based on the α-OFDM concept are proposed. α-OFDM allows to exploit large bandwidths to obtain outage gains for bursty OFDM systems. α-OFDM requires a minor change compared to OFDM which offers no capacity improvement in its actual form. Nevertheless, α-OFDM provides a way to exploit reusable frequency bands and shows outage capacity improvement compared to the classical OFDM modulation. In multicell scenarios, α-OFDM can be exploited to mitigate intercell interference. Also schemes based on α-OFDM can be used to efficiently replace extra antennas at the transmitter. A large set of applications is derived from α-OFDM, such as α-LTE, a novel evolution of LTE standard which shows performance gain in packet-switched mode and short channel delay spread. α-OFDM coupled to channel sensing methods also fits future cognitive systems which smartly exploit the available bandwidth.

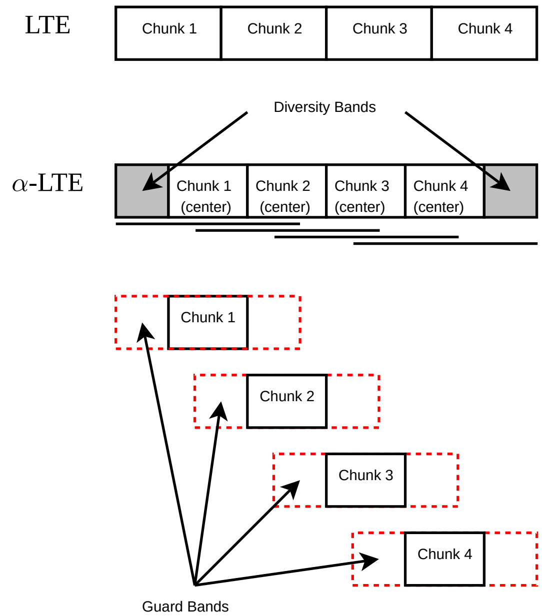

Fig. 7. α-LTE

VII. Acknowledgement

The work of was supported partially by the European Commission in the framework of the FP7 Network of Excellence in Wireless COMmunications NEWCOM++.

References

[1] ANSI/IEEE Std 802.11, 1999 Edition (R2003), http://standards.ieee.org/getieee802/download/802.11-1999.pdf

[2] "Air Interface for Fixed and Mobile Broadband Wireless Access Systems", http://standards.ieee.org/getieee802/download/802.16e-2005.pdf

[3] http://www.3gpp.org/Highlights/LTE/LTE.htm

[4] C. E. Shannon, "A Mathematical Theory of Communication", The Bell System Technical Journal, Vol. 27, pp. 379-423, 623-656, July, October, 1948.

[5] P. Viswanath, D. Tse and R. Laroia, "Opportunistic beamforming using dumb antennas", IEEE International Symposium on Information Theory. IEEE. 2002, pp.449

[6] R. Müller, R. Bains, J. Aas, "Compact MIMO Receive Antennas", Invited for 43rd Annual Allerton Conference on Communications, Control and Computing, Monticello, IL, U.S.A., September 2005.

[7] J.A. Bingham, "Multicarrier modulation for data transmission: An idea whose time has come," IEEE Commun. Mag., vol. 28, pp. 5-14, May 1990.

[8] R. M. Gray, "Toeplitz and Circulant Matrices: A Review", Now Publishers, Norwell, Massachusettsi, 1977.

[9] Ericsson, Nokia, Motorola, Rohde & Schwarz, "Proposal for LTE channel models", TSG-RAN WG4 meeting #43, R4-070572, Kobe, Japan, 7-11 May, 2007.

[10] J. Mitola, and Jr GQ Maguire, "Cognitive radio: making software radios more personal", Personal Communications, IEEE [see also IEEE Wireless Communications] 6(4), 13-18, 1999.

[11] E. Biglieri, J. Proakis, and S. Shamai, "Fading channels: Information-theoretic and communications aspects," IEEE Trans. on Inf. Theory, vol. 44, no. 6, pp. 2619-2692, Oct 1998.

[12] A. Dammann and S. Kaiser, "Performance of low complex antenna diversity techniques for mobile OFDM systems", in Proceedings 3rd International Workshop on Multi-Carrier Spread-Spectrum & Related Topics (MC-SS 2001), Oberpfaffenhofen, Germany, pages 53-64, Sept. 2001

[13] R. Couillet, M. Debbah, "Flexible OFDM systems for bursty mobile networks", *To be published*.